A New Cluster of Galaxies towards the Galactic Bulge, Suzaku J1759−3450

Hideyuki MORI,[1] Yoshitomo MAEDA,[2] Akihiro FURUZAWA,[3] Yoshito HABA,[4] and Yoshihiro UEDA,[5]

[1]*Kobayashi-Maskawa Institute for the Origin of Particles and the Universe, Nagoya University, Furo-cho, Chikusa-ku, Nagoya, 464-8602*
[2]*Department of Space Astronomy and Astrophysics, Institute of Space and Astronautical Science (ISAS), Japan Aerospace Exploration Agency (JAXA), 3-1-1, Yoshinodai, Chuo-ku, Sagamihara, 252-5210*
[3]*Institute of Liberal Arts and Sciences, Nagoya University, Furo-cho, Chikusa-ku, Nagoya, 464-8602*
[4]*Aichi University of Education, 1, Hirosawa, Igaya-cho, Kariya, 448-8542*
[5]*Department of Astronomy, Graduate School of Science, Kyoto University, Sakyo-ku, Kyoto, 606-8502*
mori@u.phys.nagoya-u.ac.jp

Abstract

We observed an extended X-ray source designated as Suzaku J1759−3450 with the Suzaku and Chandra observations towards 1RXS J175911.0−344921, which is an unidentified X-ray source listed in the ROSAT Bright Source Catalogue. A conspicuous emission line at 6 keV was also found in the Suzaku J1759−3450 spectrum. Assuming the emission line to be K emission from He-like Fe ions, we inferred Suzaku J1759−3450 to be an extragalactic object located at $z = 0.13$. The radial profile of the surface brightness in the 0.5–10 keV band was explained well with an isothermal β-model of $r_{\rm c} = 1\rlap{.}{'}61$ and $\beta = 0.78$. The X-ray spectrum was well reproduced by an optically-thin thermal plasma with the electron temperature of $kT_{\rm e} = 5.3$ keV attenuated by the photoelectric absorption of $N_{\rm H} = 2.3 \times 10^{21}$ cm^{-2}. The bolometric X-ray luminosity of $L_{\rm X}(r < r_{500}) = 4.3 \times 10^{44}$ erg s^{-1} is consistent with that expected from the $L_{\rm X}$–T relation of clusters of galaxies. In terms of the spatial extent, the X-ray spectrum, and the bolometric luminosity of the X-ray emitting gas, we concluded that Suzaku J1759−3450 is a new cluster of galaxies.

Key words: X-rays: galaxies: clusters₁ — X-rays: individual (1RXS J175911.0−344921)₂ — X-rays: individual (Suzaku J1759−3450)₃

1. Introduction

Population studies of X-ray sources are vital for our understanding of the dynamical and chemical evolution of the host galaxies since the luminous X-ray sources reflect the current activities or endpoints of the high-mass stars. Many long-exposure observations were dedicated to elucidating the X-ray population in our Galaxy such as ASCA Galactic Plane Survey (Sugizaki et al. 2001), XMM-Newton Galactic Plane Survey (Motch et al. 2010), and ChaMPlane (Grindlay et al. 2005). These extensive observing campaigns had the advantage of detecting extremely faint X-ray sources, which has never been achieved for the extragalactic X-ray surveys. Nevertheless, the sky coverage for the Galaxy is limited due to the deep pointing observations.

Hence, the more effective approach is probably required to decipher the discrete X-ray population of the Galactic components – Galactic center, disk, and bulge. Because of the most recent survey which had completed a full sky coverage with an imaging X-ray optics, the ROSAT All-Sky Survey (RASS) provides the useful database to study the X-ray population with the flux limit down to $\sim 10^{-12}$ erg s^{-1} cm^{-2}. The RASS detected many unidentified X-ray sources towards the Galactic bulge where the interstellar medium in the line of sight does not hamper the soft X-rays in the ROSAT PSPC band (0.1–2.4 keV). This fact motivates us to carry out the follow-up observations to investigate their nature (e.g., Mori et al. 2012). In the present paper, we report the X-ray properties of the cluster of galaxies newly detected with such an X-ray observation.

The paper is organized as follows; we first present the observations with Suzaku and Chandra in section 2. The X-ray data analysis is explained in section 3. After the discussion (section 4), we give a short summary of the source identification in section 5. Throughout the paper, we used the cosmological parameters of $H_0 = 70$ km s^{-1} Mpc^{-1}, $\Omega_{\rm M} = 0.27$, and $\Omega_\lambda = 0.73$, which represent the Hubble constant, dimensionless density parameters of the matter and dark energy, respectively. We also note that the errors represent the 90% confidence limit, unless otherwise mentioned.

2. Observation and data reduction

1RXS J175911.0−344921 was first discovered by the RASS. The full information of the source is described in the RASS Bright Source Catalogue (RBSC: Voges et al. 1999). The source position was $(RA, Dec)_{\rm J2000.0} = (17^{\rm h}59^{\rm m}11\rlap{.}^{\rm s}0, -34°49'21\rlap{.}{''}5)$ with an uncertainty of $32''$, which corresponds to $(l, b) = (356\rlap{.}°3818, -5\rlap{.}°4660)$ in Galactic coordinates. The count rate and the net exposure of the source is 0.12 ± 0.03 counts s^{-1} and 196 s, respectively. Assuming an absorbed power-law spectrum with $\Gamma = 2$ and $N_{\rm H} = 2.3 \times 10^{21}$ cm^{-2}, this count rate corresponds to the X-ray flux of 1.7×10^{-12} erg s^{-1} cm^{-2} in the 0.1–2.4 keV band. Since the nature of the source is still unclear, we conducted the Suzaku and Chandra observations to obtain the hard (> 2 keV) X-ray spectrum.

Table 1. Observation log

	Obs. ID	Start time (UT)	End time (UT)	Exposure[*]
Chandra	12946[†]	2011/10/13 18:22:25	2011/10/13 19:54:51	3.50 (ACIS-S3)
Suzaku	406019010	2012/03/07 21:40:15	2012/03/08 21:54:13	40.2 (XIS), 34.7 (HXD)

[*] Effective exposure of the screened data. The HXD exposure is dead-time corrected.

[†] Sequence number is 900978.

Suzaku (Mitsuda et al. 2007), the 5th Japanese-U.S. collaborated mission, enables us to perform imaging spectroscopy in the 0.2–10 keV band with the combination of the X-ray Telescopes (XRTs: Serlemitsos et al. 2007) and the X-ray Imaging Spectrometer (XIS: Koyama et al. 2007). The XIS consists of four charge-coupled devices (CCDs); three of which are front-illuminated (FI) CCDs (XIS0, 2, 3), and the other is a back-illuminated (BI) one (XIS1). The XIS2 has malfunctioned since November 9, 2006, and then we can use the two FI CCDs for the observation. A fraction of the imaging area of the XIS0 has also been unusable since June 23, 2009[1]. In this observation, the XIS was operated with the normal mode without any window options, and the spaced-row charge injection (Uchiyama et al. 2009) was applied.

Suzaku is also equipped with the non-imaging detector which covers the hard X-ray band of 10–700 keV. This detector, called Hard X-ray Detector (HXD: Takahashi et al. 2007, Kokubun et al. 2007), is composed of the Si-PIN photodiodes and the scintillators utilizing the Gadolinium Silicate crystals. The HXD was also operated with the normal mode. We performed the pointing observation where the aim point of $(RA, Dec)_{J2000.0} = (17^{h}59^{m}11\overset{s}{.}0, -33°49'21'')$ was placed on the center of the XIS field of view (FOV). We list the observation log in table 1.

We analyzed the cleaned event data provided from the Suzaku team. The data were processed with the standard pipeline with the version of 2.7.16.32. The data during the passage of the South Atlantic Anomaly (SAA) were discarded. The data obtained with the low earth elevation and day-earth elevation were also excised because of the increase in the non-X-ray background (NXB). For the XIS1, the amount of the injected charge was increased from 2 keV to 6 keV in 2011 June. Since this change also causes the increase in the NXB, we removed the events in the 2nd trailing rows[2]. We used the XSELECT ver 2.4b provided from the HEASOFT package (version 6.12) to extract the image, light curve, and spectrum. The redistributed matrix file (RMF) and ancillary response file (ARF) were made by xisrmfgen and xissimarfgen (Ishisaki et al. 2007), respectively. On the other hand, we made use of the HXD background and response files provided from the HXD team; the NXB file we used was ae406019010_hxd_pinbgd.evt.gz (tuned; Fukazawa et al. 2009), and the response file was ae_hxd_pinxinome11_20110601.rsp.

Chandra (Weisskopf et al. 2000) is the U.S. flagship mission for X-ray astronomy. Chandra possesses the X-ray telescopes and attitude control system, called High Resolution Mirror Assembly (HRMA: van Speybroeck et al. 1997), al-lowing to obtain X-ray images with the unprecedented high-angular resolution. On its focal plane, the Advanced CCD Imaging Spectrometer (ACIS: Burke et al. 1997) is placed to provide imaging spectroscopy. The ACIS contains 10 CCD chips; a fraction of these CCDs makes a 2×2 CCD array (ACIS-I) and the others do 1×6 CCD array (ACIS-S). The primary goal of the Chandra observation we proposed is to determine the accurate position of 1RXS J175911.0−344921. Thus, only the ACIS-S3 chip was turned on. Moreover, we selected the 128-pixel subarray mode to avoid the pile-up effect. The observation was performed with the very faint mode. The grating modules were not used. The log of the Chandra observation is also summarized in table 1.

We used the level 2 event file for the analysis; the standard data processing was applied to the data. In order to generate the X-ray image and spectrum described below, the Chandra Interactive Analysis of Observations (CIAO, version 4.4: Fruscione et al. 2006)[3] and the relevant calibration files (CALDB, version 4.4.6) were utilized.

3. Analysis

3.1. X-ray image and light curve

Figure 1a shows the XIS image in the 0.5–10 keV band of 1RXS J175911.0−344921. From each CCD sensor, we made an X-ray image binned by a factor of 4. After the subtraction of the NXB image created with xisnxbgen (Tawa et al. 2008), the vignetting correction was applied to each image. We estimated the vignetting effect of the Suzaku XRT for a uniform sky with xissim. These corrected images were added together and then smoothed with a Gaussian function of $\sigma = 0\overset{'}{.}28$. We also show the X-ray image in the 0.5–8 keV band obtained with the Chandra ACIS-S3 chip in figure 1b. After the 4×4 pixel binning, the smoothing with a Gaussian function of $\sigma = 7\overset{''}{.}9$ was applied to the image.

The XIS image clearly shows extended emission located $\sim 1'$ away from the position of 1RXS J175911.0−344921 (green cross point in figure 1a) in the south-east direction. The emission has a nearly circular shape with a radius of $\sim 4'$. A point-like source was marginally found at $(RA, Dec)_{J2000.0} = (17^{h}59^{m}47\overset{s}{.}0, -34°49'28\overset{''}{.}3)$. The source is positionally co-incident with two radio sources, MOST 1756−348 and PMN J1759−3449, within an uncertainty of $15''$. Thus, the source may be an X-ray counterpart of either of these radio sources. However, the detailed study on the source is beyond the scope of this paper. We also mention that there was no X-ray source at $(RA, Dec)_{J2000.0} = (17^{h}59^{m}11\overset{s}{.}0, -34°49'21\overset{''}{.}5)$ in the Chandra ACIS image. Thus, we pay attention to this diffuse emission, designated as Suzaku J1759−3450 hereafter, as an

---

[1] Suzaku memo: JX-ISAS-SUZAKU-MEMO-2010-01

[2] http://www.astro.isas.ac.jp/suzaku/analysis/xis/xis1_ci_6_nxb/

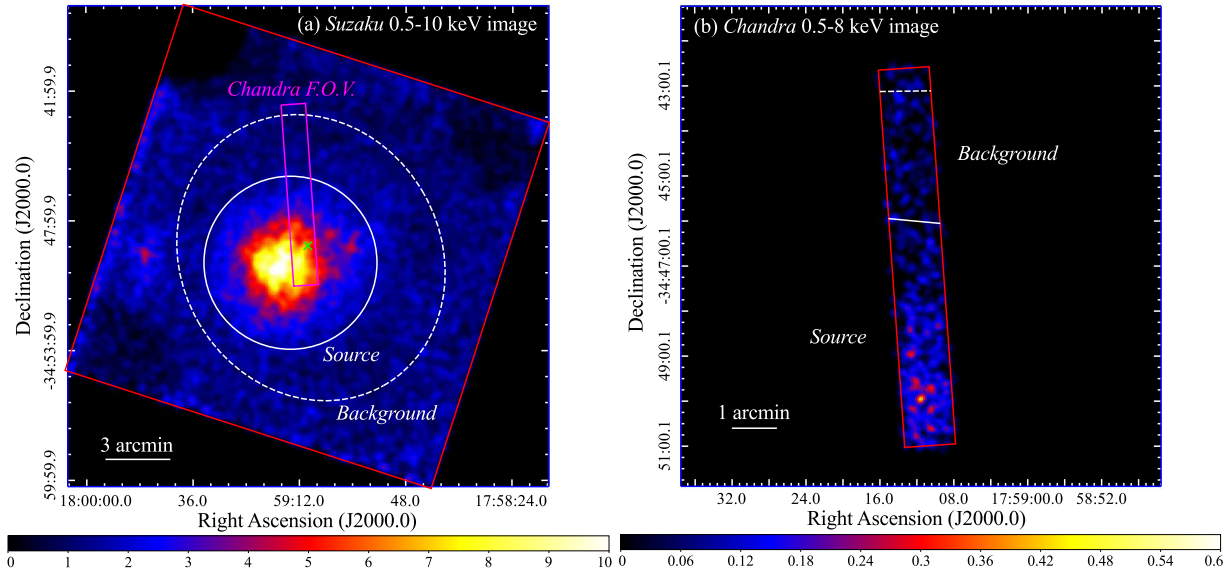[3] http://cxc.harvard.edu/ciao/

Fig. 1. Suzaku XIS image in the 0.5–10 keV band (a) and Chandra ACIS-S3 image in the 0.5–8 keV band (b) of 1RXS J175911.0−344921. The XIS image was binned with 4×4 pixels and then smoothed with the Gaussian kernel of $\sigma = 0'.28$. The subtraction of the Non-X-ray background and the vignetting correction were applied to the XIS image. The source and background regions to extract the XIS spectra are indicated with white solid circle and dashed ellipse, respectively. The red square and magenta rectangle represent the XIS and ACIS-S3 field of views, respectively. The position of 1RXS J175911.0−344921 is shown by a green cross. The ACIS-S3 was operated in the 128-pixel subarray mode. We made a zoomed-up image with the binning of 4×4 pixels. The smoothing with the Gaussian kernel of $\sigma = 7''.9$ was also applied. The white solid and dashed curve represent a part of the source and background regions in the XIS image, which are overlapped with the ACIS-S3 field of view (red square). The color scales at the bottom of these panels are in unit of photons per $4''.2 \times 4''.2$ (a) and $2''.0 \times 2''.0$ (b) image pixel.

X-ray counterpart of the RBSC source.

First, we searched for time variability of the source intensity. For the source-extraction region, we defined a circle with a radius of $4'$ where the surface brightness decreases to $\sim 10\%$ of its peak (a white solid circle in figure 1a). The center of the source region is at $(RA, Dec)_{\rm J2000.0} = (17^{\rm h}59^{\rm m}14^{\rm s}.02, -34°49'56''.7)$. The background region was chosen to be an ellipse excluding the source region, shown by a white dashed ellipse in figure 1a. The radii of the ellipse along the major and minor axes are $6'.8$ and $6'$, respectively. It is well known that there is diffuse X-ray emission with characteristic Fe-K emission lines towards the Galactic plane (Galactic Ridge X-ray Emission (GRXE): Koyama et al. 1986). Since the X-ray intensity of this diffuse emission has a spatial dependence (e.g., Yamauchi & Koyama 1993, Kokubun et al. 2001, Revnivtsev 2003), we aligned the axes of the ellipse to the Galactic longitude and latitude to mitigate the spatial variability of the GRXE. The size of the ellipse was determined so as to avoid the detector corners illuminated by the calibration sources, anomalous rectangular region in XIS0, and the eastern point source. We made the background-subtracted XIS light curve for each CCD sensor, and then fitted the light curves with a constant model. All the fits were acceptable with $\chi^2_\nu = 1.1$–1.3. The average count rates were 0.153 ± 0.004 cts s^{-1} for XIS0, 0.188 ± 0.005 cts s^{-1} for XIS1, and 0.173 ± 0.004 cts s^{-1} for XIS3.

We also made a hard X-ray light curve from the HXD-PIN data. The deadtime-corrected count rate in the 18–40 keV band was 0.140 ± 0.004 cts s^{-1}, while the NXB count rate derived from the "tuned" background file was 0.142 ± 0.001 cts s^{-1}. This indicates that there is no significant X-ray emission above 10 keV within the HXD-PIN FOV. Hence, we ignored the HXD-PIN data in the spectral analysis.

To examine the spatial extent of the source quantitatively, we generated a radial profile of the surface brightness from the XIS image without the NXB subtraction and the vignetting correction, shown in figure 2. The origin of the radial profile was set to be $(RA, Dec)_{\rm J2000.0} = (17^{\rm h}59^{\rm m}17^{\rm s}.41, -34°50'18''.6)$, the position of the peak brightness. The surface brightness profile of SS Cyg (black dashed line in figure 2), which corresponds to the point spread function (PSF) of the XRTs, was plotted as well to illustrate the diffuse emission. We normalized the peak brightness of SS Cyg to that of Suzaku J1759−3450.

We tried to reproduce the surface brightness profile of Suzaku J1759−3450, $S(r)$, with a single β-model (Cavaliere & Fusco-Femiano 1976). The β-model is frequently applied to a self-gravitating system and is given by $S(r) \propto (1 + (r/r_{\rm c})^2)^{-3\beta+1/2}$, where $r_{\rm c}$ and β represent a core radius and a power-law index, respectively. Because of the point-like source located in the eastern direction of Suzaku J1759−3450, we excised the outskirt of the radial profile ($r > 5'$) from the fit.

Since the XRT PSF and the vignetting effect are convolved in the radial profile, we evaluated β and $r_{\rm c}$ as described below. First, we created a sky image which surface brightness is given by a β-model of $(\beta, r_{\rm c})$. The peak brightness was set to be at $(RA, Dec)_{\rm J2000.0} = (17^{\rm h}59^{\rm m}17^{\rm s}.41, -34°50'18''.6)$. Assuming that the X-ray emitting gas is an isothermal optically-thin plasma with the temperature of $kT_{\rm e} \sim 5$ keV and
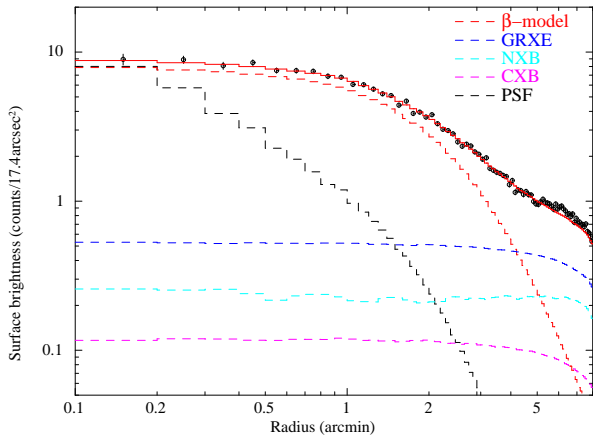
Fig. 2. Radial profile of the surface brightness of Suzaku J1759−3450 in the 0.5–10 keV band (open circles). The error bar on each data shows a 1σ statistical uncertainty. The black dashed line represents the surface brightness profile of SS Cyg, in which its brightness peak was normalized to that of Suzaku J1759−3450. The best-fit β-model with $(\beta, r_{\rm c}) = (0.78, 1\!'.61)$, GRXE, NXB, and CXB components are shown with red, blue, cyan, and magenta dashed lines, respectively. The red solid line indicates the combined model of these components.

that the X-ray emission is modified with a foreground absorption of $N_{\rm H} = 2.3 \times 10^{21}$ cm^{-2}, we simulated the XIS events using `xissim`. The exposure time and photon flux were set to be large enough to obtain sufficient photon statistics. Using the simulated event list, we again made an X-ray image and a radial profile of the surface brightness ($S_{\beta}(r)$) in the same manner described above. Then, the peak brightness was normalized to be unity.

The X-ray emission from Suzaku J1759−3450 is contaminated by some celestial and instrumental background components: GRXE, Cosmic X-ray Background (CXB), and NXB. The contribution of the NXB, $S_{\rm NXB}(r)$, was estimated by generating the surface brightness profile from the NXB image. In order to estimate the CXB and GRXE contributions, denoted by $S_{\rm CXB}(r)$ and $S_{\rm GRXE}(r)$, respectively, we again simulated the XIS events assuming a uniform sky with a radius of $20'$. The procedure for deriving $S_{\rm CXB}(r)$ or $S_{\rm GRXE}(r)$ was the same as that of $S_{\beta}(r)$. The CXB spectrum was assumed to be a power-law model with a cutoff energy of 40 keV (Boldt 1987). The exposure time was set to be the same as that of the observation.

On the other hand, for the GRXE component, we extracted the X-ray spectrum from the outside of the background region (dashed ellipse in figure 1a). To remove the contribution of the eastern point-like source, a circle with a radius of $2'$ centered on the source was excluded from the extraction region. After the NXB subtraction, we fitted the spectrum with a phenomenological model: an optically-thin thermal plasma model with two different temperatures, referred to as Uchiyama et al. (2013), plus the CXB model described above. The absorption column density was fixed to be $N_{\rm H} = 2.3 \times 10^{21}$ cm^{-2} again. The best-fit parameters of the plasma temperatures were 0.24 keV and 7.4 keV. Uchiyama et al. (2013) also derived the (l, b)-dependence of the GRXE intensity. The X-ray flux of the plasma component in the 2.3–8 keV band was $7.2 \times$

10^{-4} photons s^{-1} cm^{-2}, consistent with that estimated from the equation (1) in Uchiyama et al. (2013) (7.0×10^{-4} photons s^{-1} cm^{-2}). Hence, our evaluation of the GRXE spectral model and its photon flux was verified. The exposure time in the GRXE simulation was set to be 2000 times larger than that of the observation to reduce the statistical fluctuation.

We fitted the radial profile of Suzaku J1759−3450 in the range of $0\!'.1$–$5\!'.0$ with a combined model of these components as follows: $S(r) = a \times S_{\beta}(r) + S_{\rm GRXE}(r) + S_{\rm CXB}(r) + S_{\rm NXB}(r)$. Here a represents the normalization of the β-model component. For a given $(\beta, r_{\rm c})$, the χ^2 value was calculated from the best-fit parameters of a. We examined the appropriate β and $r_{\rm c}$ which yield the χ^2 minimum by searching the parameter space constructed from a set of $(\beta, r_{\rm c})$. Since the β and $r_{\rm c}$ were strongly correlated with each other, the unique determination of $(\beta, r_{\rm c})$ was difficult. Therefore, we adopted the parameter combination of $(\beta, r_{\rm c}) = (0.78, 1\!'.61)$, which gave an acceptable fit of $\chi^2 = 58/50$ d.o.f.. The confidence contours of $(\beta, r_{\rm c})$ is shown in figure 3.
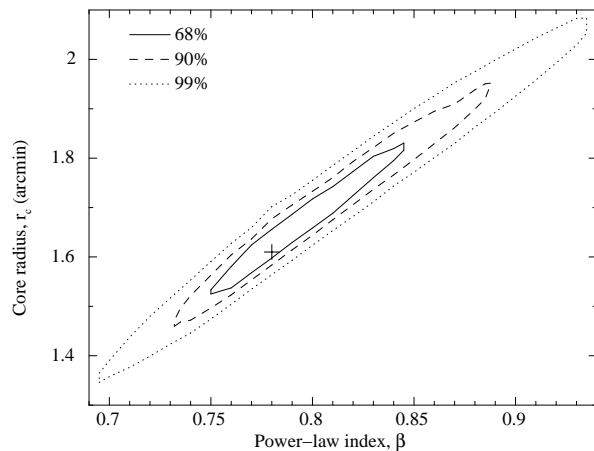

Fig. 3. Confidence contours of β and the core radius. The solid, dashed, and dotted lines represent the 68% ($\Delta\chi^2 = 2.30$), 90% ($\Delta\chi^2 = 4.61$), and 99% ($\Delta\chi^2 = 9.21$) confidence levels, respectively. The parameter set of $(\beta, r_{\rm c}) = (0.78, 1\!'.61)$ we adopted here is shown by a cross.

3.2. Spectral analysis

We extracted the source and background spectra for each CCD sensor from the respective regions shown in figure 1a. We made the averaged spectrum for the FI CCDs. The ARF was made by `xissimarfgen` assuming the X-ray surface brightness derived in the previous section: a single β-model with $(\beta, r_{\rm c}) = (0.78, 1\!'.61)$. For the XIS1, the 2nd trailing rows were excluded from the ARF calculation. Figure 4a shows the XIS spectra.

We found a conspicuous line-like emission at ~ 6 keV. Although there were some subtle structures over the whole energy band, we first tried to fit the spectra with a power-law continuum plus Gaussian emission line attenuated by photoelectric absorption (Balucinska-Church & McCammon 1992). The σ of the Gaussian function was fixed to be 0. Taking into the consideration the uncertainty of the relative normalization
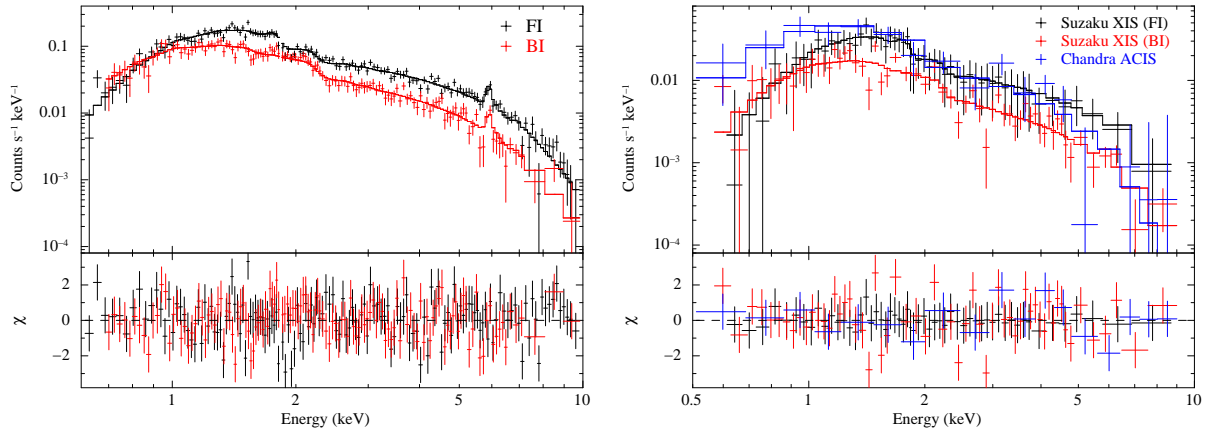
Fig. 4. X-ray spectra of Suzaku J1759−3450 obtained with the Suzaku XIS (a) and the Chandra ACIS-S3 (b). In the panel (b), the XIS spectra extracted from the Chandra source region (see figure 1b) are also shown. The spectra of the FI and BI CCDs are represented with black and red pluses, while the Chandra spectrum is done with blue pluses. In order to increase the photon statistics of the FI spectrum, we took an average of the XIS0 and XIS3 spectra. The best-fit optically-thin thermal plasma models are overlaid with solid curves.

between FI and BI CCDs, we multiplied the spectra by a constant factor; the factor of the FI spectrum was fixed to be unity and that of the BI spectrum was free parameter. We excluded the 1.82–1.84 keV band from the spectral fit due to the uncertainty of the quantum efficiency around the Si edge.

This model yielded a marginally acceptable fit with $\Gamma = 2.1$ and $N_{\mathrm{H}} = 3.8 \times 10^{21}$ cm^{-2} ($\chi^2 = 346/273$ d.o.f.). Thus, we introduced an exponential cutoff in the power-law continuum. The cutoff energy of ~ 5 keV improved the fit significantly ($\chi^2 = 315/272$ d.o.f.). The presence of the exponential cutoff implies that the continuum emission has a thermal origin. We then replaced the cutoff power-law model with a thermal bremsstrahlung. The absorbed bremsstrahlung model including the Gaussian emission line gave again an acceptable fit of $\chi^2 = 315/273$ d.o.f.. The electron temperature and the absorption column density were $kT_{\mathrm{e}} = 5.0^{+0.4}_{-0.3}$ keV and $N_{\mathrm{H}} = (2.1 \pm 0.3) \times 10^{21}$ cm^{-2}, respectively. The center energy of the emission line was found to be $5.91^{+0.02}_{-0.03}$ keV.

The emission line at ~ 6 keV indicates that the X-ray emitting gas is not in the local universe. Hence, we tried to fit the spectra by absorbed thermal emission from an optically-thin plasma in collisional ionization equilibrium (APEC in XSPEC) with the redshift parameter thawed. The elemental abundance relative to the solar value (Anders & Grevesse 1989) was also set to be free parameter. Again, we obtained an acceptable fit ($\chi^2 = 311/273$ d.o.f.). The best-fit model and parameters are shown in figure 4a and table 2, respectively. The absorption column density of $N_{\mathrm{H}} = (2.3 \pm 0.3) \times 10^{21}$ cm^{-2} and the electron temperature of $kT_{\mathrm{e}} = 5.3^{+0.5}_{-0.3}$ keV were consistent with those obtained by the bremsstrahlung model. The elemental abundance was determined to be $Z/Z_{\odot} = 0.18 \pm 0.05$. The redshift parameter was found to be $z = 0.132^{+0.005}_{-0.003}$, implying that the center energy of the emission line at the rest frame is 6.7 keV. Thus, the emission line is identified with Kα emission from helium-like Fe ions (Fe XXV). We note that the spectral model and its best-fit parameters were consistent with those assumed in the analysis of the surface brightness profile (see section 3.1). Hence, the self-consistency for the estimation of

Table 2. Best-fit parameters of the Suzaku J1759−3450 spectra*.

Parameters	Source	Chandra region
N_{H} (10^{21} cm^{-2})	2.3 ± 0.3	2.3 (fixed)
kT_{e} (keV)	$5.3^{+0.5}_{-0.3}$	$6.3^{+1.5}_{-1.2}$
$Z/Z_{\odot}$	0.18 ± 0.05	0.18 (fixed)
Redshift z	$0.132^{+0.005}_{-0.003}$	0.132 (fixed)
Flux (erg s^{-1} cm^{-2})†	4.6×10^{-12}	—
χ^2/d.o.f.	$311/273 = 1.1$	$104/128 = 0.8$

* Superscript and subscript figures represent the upper and lower limit of the 90% confidence interval, respectively.
† In the 0.5–10 keV band.

(β, r_{c}) was verified.

3.2.1.   Chandra spectrum

The Chandra observation covered only a small fraction of the Suzaku FOV since we applied the window option with a width of 128 pixel. Nevertheless, we found the X-ray emission from Suzaku J1759−3450 within the Chandra FOV. (see figure 1b). Then, we extracted the spectrum from the source region where the Chandra FOV and the source region of the XIS spectra (see section 3.1) overlap. The background spectra was also generated from the overlapping background region, defined in the same manner as the source region. The background-subtracted spectrum was grouped to contain at least 15 photons per bin.

We show the Chandra spectrum of Suzaku J1759−3450 in figure 4b. Since the net count of the spectrum is only 217 photons, the spectrum did not provide sufficient constraints on the spectral parameters of the diffuse emission. Hence, we created the XIS spectra from this source region shown by black and red pluses in figure 4b, and then performed a joint fit to the Chandra and Suzaku spectra. For the XIS spectra, the background spectra used in the previous section were subtracted to minimize the statistical uncertainty.

We fitted these spectra with the thermal plasma model (APEC in XSPEC) multiplied by photoelectric absorption. In this fit, we fixed the parameters of the absorption column density (N_{H}), the elemental abundance, and redshift (z) to be those

derived from the Suzaku spectra; the electron temperature and the normalization were free parameters. The absorbed thermal plasma model gave an acceptable fit ($\chi^2 = 104/128$ d.o.f.). The best-fit electron temperature was $6.3^{+1.5}_{-1.2}$ keV (see also table 2). The temperature was consistent with that of the X-ray emission extracted from the Suzaku source region.

4. Discussion

We conducted the Chandra and Suzaku observations of 1RXS J175911.0−344921 to perform the imaging spectroscopy above 2 keV for the first time. No point-like X-ray counterpart of 1RXS J175911.0−344921 was found both in the Chandra and Suzaku FOVs. On the other hand, we found diffuse X-ray emission with a nearly circular shape, designated as Suzaku J1759−3450. The source extent of $63''$ for 1RXS J175911.0−344921 indicates extended X-ray emission compared with the ROSAT PSF towards this RBSC source. Thus, the large spatial extent may cause a false determination of the source position. The surface brightness profile and the extragalactic origin of the diffuse X-ray emission indicate that Suzaku J1759−3450 is a new cluster of galaxies.

The X-ray profile of the surface brightness in the 0.5–10 keV band did not show a strong central peak and was reproduced with a single β-model. The core radius and the power-law index were estimated to be $r_c = 1'.61$ and $\beta = 0.78$, respectively. The power-law index we adopted here is in the range of the β parameters obtained by Ota & Mitsuda (2004). We note that the peak position of the surface brightness at $(RA, Dec)_{\rm J2000.0} = (17^h59^m17^s41, -34°50'18''.6)$ was slightly shifted in the south-east direction from the center of the circular emission whose spectrum we extracted. The non-axisymmetric morphology suggests that the X-ray emitting gas is far from relaxed. No central cooling core also suggests that the hot gas is more likely a merging system.

The X-ray spectrum of Suzaku J1759−3450 showed a remarkable emission line at ~ 6 keV. Taking into account the cosmological redshift, we reproduced the spectrum by an optically-thin thermal plasma with an electron temperature of $kT_{\rm e} = 5.3$ keV. Since the redshift parameter was determined to be $z = 0.132$, the origin of the emission line was identified to be highly-ionized Fe. The absorption column density of $N_{\rm H} = (2.3 \pm 0.3) \times 10^{21}$ cm^{-2} was consistent with the H I column density of 2.4×10^{21} cm^{-2} (Dickey & Lockman 1990). This result reinforces that Suzaku J1759−3450 is an extragalactic object suffered from the local ($z = 0$) absorption due to the Galactic interstellar medium. The redshift parameter of $z = 0.132$ corresponds to the distance to the source of 550 Mpc. The angular separation of $1'$ on the sky is equivalent to the distance of 140 kpc. Thus, the core radius of Suzaku J1759−3450 is ~ 230 kpc.

Assuming that the hot gas of Suzaku J1759−3450 is in hydrostatic equilibrium and that its density profile follows an isothermal β-model, we can estimate the total mass of the cluster within a given radius as follows (e.g., Fabricant et al. 1980):

$$M(<r) = \frac{3\beta k T_{\rm e} r^3}{G \mu m_{\rm H} r_c^2} \frac{1}{1 + (r/r_c)^2}. \tag{1}$$

Here, k, G, $\mu = 0.6$, and $m_{\rm H}$ represent the Boltzmann constant,

the gravitational constant, the mean molecular weight, and the mass of the hydrogen, respectively. Although we assumed here that the gas was isothermal, no temperature structure was indeed found in the joint analysis of the Chandra and Suzaku spectra. Using the $(\beta, r_c) = (0.78, 1'.61)$, we estimated the total mass within $r < 4'$ to be $2.2 \times 10^{14} M_\odot$, consistent with that of a typical cluster of galaxies.

The X-ray flux in the 0.5–10 keV band of 4.6×10^{-12} erg s^{-1} cm^{-2} is converted into the luminosity of 2.1×10^{44} erg s^{-1} at $z = 0.132$. The unabsorbed bolometric luminosity is also estimated to be $L_{\rm X}(r < 4') = 3.5 \times 10^{44}$ erg s^{-1}. In order to compare our result with the $L_{\rm X}$–T relation which has been ever studied, we calculated the overdensity radius (r_{500}) within which the averaged density ($\bar{\rho}$) of the cluster is 500 times larger than the critical density of the universe ($\rho_{\rm crit} = 9.2 \times 10^{-30}$ g cm^{-3}). Since the averaged density can be evaluated by

$$\bar{\rho}(<r) = \frac{9\beta k T_{\rm e}}{4\pi G \mu m_{\rm H} r_c^2} \frac{1}{1 + (r/r_c)^2}, \tag{2}$$

we estimated to be $r_{500} = 5.5 r_c = 8'.9$, which corresponds to the distance of 1.3 Mpc. A new ARF was re-calculated with `xissimarfgen` for the source region with a radius of $8'.9$. Using the best-fit parameters derived from the spectral analysis, the resultant bolometric luminosity was estimated to be $L_{\rm X}(r < r_{500}) = 4.3 \times 10^{44}$ erg s^{-1}.

We also investigated the systematic uncertainty of the X-ray luminosity due to the β-model assumed in the ARF calculation. The two cases were taken into consideration based on the 90% confidence contour shown in figure 3: $(\beta, r_c) = (0.732, 1'.460)$ (lower limit) and $(0.888, 1'.952)$ (upper limit). The XIS spectra were re-fitted with the optically-thin thermal plasma model using the ARFs assumed in these cases. The best-fit parameters of $N_{\rm H}$, $kT_{\rm e}$, the abundance, and the redshift z were all consistent with those derived from the $(\beta, r_c) = (0.78, 1'.61)$ case. The bolometric luminosity changed by 2%: $L_{\rm X}(r < r_{500}) = 4.2 \times 10^{44}$ erg s^{-1} in the lower-limit case and 4.4×10^{44} erg s^{-1} in the upper-limit case.

According to the equation (5) in Ota et al. (2006), the expected bolometric luminosity at $kT_{\rm e} = 5.3$ keV is 1.2×10^{45} erg s^{-1}, 3 times larger than that of Suzaku J1759−3450. Taking into consideration a relatively large scatter in the $L_{\rm X}$–T relation shown in figure 5a of Ota et al. (2006), however, we should conclude that the combination of the temperature and bolometric luminosity within r_{500} of Suzaku J1759−3450 is consistent with that of a typical cluster. Suzaku J1759−3450 may be classified into relatively dim cluster of galaxies based on its luminosity. Maughan et al. (2012) argued that unrelaxed clusters of galaxies with temperature below 6 keV tend to show the X-ray luminosities lower than those of the relaxed ones. Our conjecture that Suzaku J1759−3450 is not a relaxed system supports their claim. We note that the overdensity radius of $r_{500} \sim 1$ Mpc also agrees with a hot gas associated with a cluster of galaxy, since the overdensity radius depends weakly on the redshift parameter and concentrates around 1 Mpc (e.g., Ota & Mitsuda 2002).

5. Summary

We discovered extended hard X-ray emission above 2 keV towards the unidentified X-ray source, 1RXS J175911.0−344921, with the Suzaku and Chandra observations. Thanks to the low background level, characteristic of the Suzaku's performance, the spectrum of this diffuse X-ray emission was obtained with sufficient photon statistics. We summarize the image and spectral analyses of this diffuse emission, designated as Suzaku J1759−3450, as below.

1. The radial profile of the surface brightness of Suzaku J1759−3450 was explained with the isothermal β-model. The core radius and power-law index were estimated to be $r_c = 1\overset{\prime}{.}61$ and $\beta = 0.78$, respectively.

2. The Suzaku J1759−3450 spectrum was well reproduced with the X-ray emission from an optically-thin thermal plasma with the temperature of $kT_e = 5.3^{+0.5}_{-0.3}$ keV, modified with the Galactic absorption of $N_H = (2.3 \pm 0.3) \times 10^{21}$ cm^{-2}. The emission line at ~ 6 keV was identified with the redshifted ($z = 0.132$) Kα emission from the helium-like Fe ions. The elemental abundance was 0.18 ± 0.05 relative to the solar value.

3. Assuming that the X-ray emitting gas is an isothermal sphere in hydrostatic equilibrium, the total mass of this cluster of galaxies was estimated to be $2.2 \times 10^{14} M_\odot$. The unabsorbed bolometric luminosity within r_{500} of 4.3×10^{44} erg s^{-1} was slightly lower than that expected from the electron temperature of $kT_e = 5.3$ keV and the L_X–T relation. However, the relatively large scatter in the L_X–T relation allows Suzaku J1759−3450 to be considered as a new member of cluster of galaxies.

References

Anders, E., & Grevesse, N. 1989, Geochim. Cosmochim. Acta, 53, 197

Balucinska-Church, M., & McCammon, D. 1992, ApJ, 400, 699

Boldt, E. 1987, Observational Cosmology, 124, 611

Brinkman, A. C., Gunsing, C. J., Kaastra, J. S., et al. 1997, Proc. SPIE, 3113, 181

Burke, B. E., Gregory, J. A., Bautz, M. W., et al. 1997, IEEE Transactions on Electron Devices, 44, 1633

Canizares, C. R., Davis, J. E., Dewey, D., et al. 2005, PASP, 117, 1144

Cavaliere, A., & Fusco-Femiano, R. 1976, A&A, 49, 137

Dickey, J. M., & Lockman, F. J. 1990, ARA&A, 28, 215

Fabricant, D., Lecar, M., & Gorenstein, P. 1980, ApJ, 241, 552

Fruscione, A., et al. 2006, Proc. SPIE, 6270

Fukazawa, Y., et al. 2009, PASJ, 61, 17

Grindlay, J. E., Hong, J., Zhao, P., et al. 2005, ApJ, 635, 920

Ishisaki, Y., et al. 2007, PASJ, 59, 113

Kokubun, M., Makishima, K., Sakano, M., Yamauchi, S., & Ebisawa, K. 2001, New Century of X-ray Astronomy, 251, 304

Kokubun, M., et al. 2007, PASJ, 59, 53

Koyama, K., Makishima, K., Tanaka, Y., & Tsunemi, H. 1986, PASJ, 38, 121

Koyama, K., et al. 2007, PASJ, 59, 23

Maughan, B. J., Giles, P. A., Randall, S. W., Jones, C., & Forman, W. R. 2012, MNRAS, 421, 1583

Mitsuda, K., Bautz, M., Inoue, H., et al. 2007, PASJ, 59, 1

Mori, H., Maeda, Y., Ueda, Y., Dotani, T., & Ishida, M. 2012, PASJ, 64, 112

Motch, C., et al. 2010, A&A, 523, A92

Ota, N., & Mitsuda, K. 2002, ApJL, 567, L23

Ota, N., & Mitsuda, K. 2004, A&A, 428, 757

Ota, N., Kitayama, T., Masai, K., & Mitsuda, K. 2006, ApJ, 640, 673

Predehl, P., Braeuninger, H. W., Brinkman, A. C., et al. 1997, Proc. SPIE, 3113, 172

Revnivtsev, M. 2003, A&A, 410, 865

Serlemitsos, P. J., et al. 2007, PASJ, 59, 9

Sugizaki, M., Mitsuda, K., Kaneda, H., Matsuzaki, K., Yamauchi, S., & Koyama, K. 2001, ApJS, 134, 77

Takahashi, T., et al. 2007, PASJ, 59, 35

Tawa, N., et al. 2008, PASJ, 60, 11

Uchiyama, H., et al. 2009, PASJ, 61, 9

Uchiyama, H., Nobukawa, M., Tsuru, T. G., & Koyama, K. 2013, PASJ, 65, 19

van Speybroeck, L. P., Jerius, D., Edgar, R. J., et al. 1997, Proc. SPIE, 3113, 89

Voges, W., et al. 1999, A&A, 349, 389

Weisskopf, M. C., Tananbaum, H. D., Van Speybroeck, L. P., & O'Dell, S. L. 2000, Proc. SPIE, 4012, 2

Yamauchi, S., & Koyama, K. 1993, ApJ, 404, 620